

Indolizino[1,2-*b*]quinolines Derived from A–D Rings of Camptothecin: Synthesis and DNA Interaction

AURORE PERZYNA^a, RAYMOND HOUSSIN^a, JEAN-FRANÇOIS GOOSSENS^a, NICOLE POMMERY^a,
CARINE MARTY^b, MICHAEL FACOMPRÉ^b, PIERRE COLSON^c, CLAUDE HOUSSIER^c, CHRISTIAN BAILLY^b and
JEAN-PIERRE HÉNICHART^{a,*}

^aInstitut de Chimie Pharmaceutique Albert Lespagnol, EA 2692, Université de Lille 2, BP 83, 59006 Lille, France; ^bINSERM U-524 et Laboratoire de Pharmacologie Antitumorale du Centre Oscar Lambret, IRCL, Place de Verdun, 59045 Lille, France; ^cUnité de Biospectroscopie, Université de Liège au Sart-Tilman, 4000 Liège, Belgium

(Received 28 June 2002; In final form 2 October 2002)

Camptothecin consists of a lactone E-ring adjacent to a tetracyclic A–D ring planar chromophore which are essential for topoisomerase I inhibition and DNA interaction, respectively. The A–D ring system can be exploited to develop DNA-binding molecules. Indolizino[1,2-*b*]quinoline derivatives substituted with a piperidinoethoxy side chain on the A-ring and an aminomethyl function on the D one were synthesized and their DNA-binding properties and *in vitro* cytotoxicity investigated.

Keywords: Camptothecin, Indolizino[1,2-*b*]quinolines, DNA binding

INTRODUCTION

Mappicine ketone¹ (MPK) is an analogue of mappicine, a plant alkaloid isolated from *Mappia foetidia* Miers (Figure 1). MPK has been identified as an antiviral lead compound^{2,3} with selective activity against herpes viruses HSV-1, HSV-2 and human cytomegalovirus but its mechanism of action has not been determined. The skeleton of mappicine is a tetracyclic indolizino[1,2-*b*]quinoline, which is also present in camptothecin.

Camptothecin (CPT) is another natural product, isolated from *Camptotheca acuminata*⁴ (Figure 1). CPT has a pentacyclic structure and is a powerful antitumoral agent. CPT inhibits topoisomerase I, an essential enzyme involved in transient scission and

religation of DNA during replication and transcription phases.⁵ Binding of CPT to the topoisomerase I-DNA complex and interference with the religation step of this process was recognized as the primary mechanism of action of CPT. In the ternary complex, CPT makes direct interactions with the double helix at the cleavage site. Different models have been proposed for the configuration of this complex^{6–10} and in all cases, the indolizino[1,2-*b*]quinoline scaffold of CPT, represented by A–D rings, provides the necessary framework for DNA interaction whereas the lactone E-ring interacts essentially, if not exclusively, with the enzyme, through the Arg364 and Asp533 residues of human topoisomerase I.⁷ The skeleton of these two alkaloids is an indolizino[1,2-*b*]quinoline moiety. Thus far, all the drug design approaches in the CPT series have been oriented towards the discovery of potent topoisomerase I poisons, generally with little or no consideration of the DNA binding aspect. Here, we report a radically different approach that consisted in eliminating the lactone E-ring, therefore prohibiting the targeting of topoisomerase I, but exploiting the indolizino[1,2-*b*]quinoline structure to develop DNA sequence-reading molecules. We report the synthesis and DNA-binding properties of six indolizino[1,2-*b*]quinoline derivatives. The designed compounds (Figure 2) lack the lactone E-ring moiety of CPT but preserve the A–D indolizino[1,2-*b*]quinoline which can be considered as the DNA-binding unit of CPT.

*Corresponding author: Institut de Chimie Pharmaceutique Albert Lespagnol, BP 83, 59006 Lille, France. Tel.: +33-3-2096-4374. Fax: +33-3-2096-4906. E-mail: henicha@phare.univ-lille2.fr

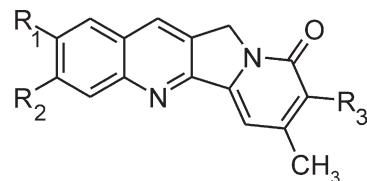
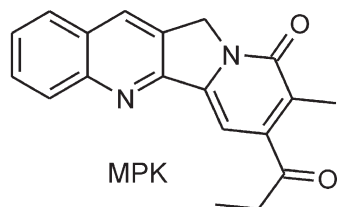


FIGURE 2 General structure of studied compounds.

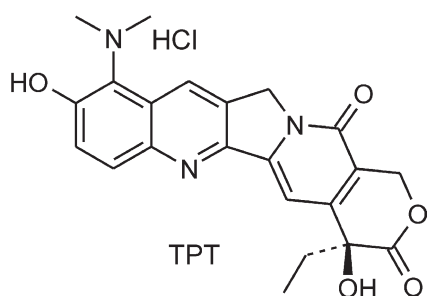
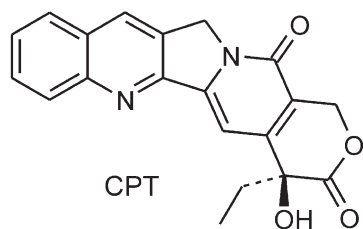
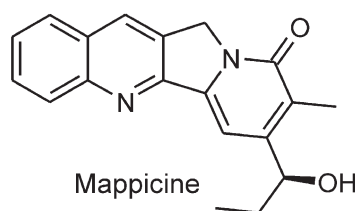


FIGURE 1 Structure of Mappicine ketone (MPK), Mappicine, Camptothecin (CPT) and Topotecan (TPT).

We investigated two types of substitutions in order to potentially promote drug-DNA interaction. On the one hand, the quinoline A ring was substituted at position-2 or -3 with a positively charged piperidine side chain liable to interact with the DNA phosphates and to improve the aqueous solubility of the corresponding molecules. On the other hand, the D ring was substituted with a methyl group at position-7 and either an aminomethyl or an amide group at position-8. These two functions were selected for their hydrogen binding capacity.

MATERIALS AND METHODS

Biochemical and Spectrophotometric Measurements

Absorption and melting temperature studies were performed as previously described.¹¹ Binding

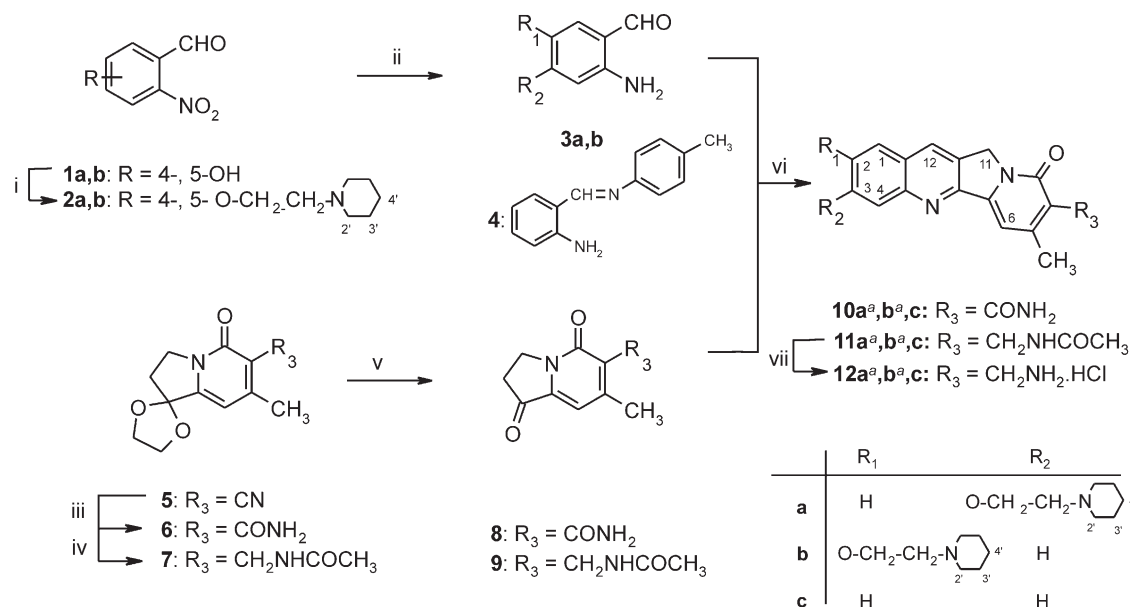
constants were determined using a competitive displacement fluorometric assay with DNA-bound ethidium.¹² Variation in melting temperature ($\Delta T_m = T_m^{\text{complex}} - T_m^{\text{DNA}}$): T_m measurements were performed in BPE buffer pH 7.1 (6 mM Na_2HPO_4 , 2 mM NaH_2PO_4 , 1 mM EDTA) using 10 μM compound and 20 μM calf thymus DNA (CT) or poly(dAdT)₂ (dAT), at 260 nm with a heating rate of 1°C/min. Briefly, solutions of 1 μM calf thymus DNA in BPE buffer (6 mM Na_2HPO_4 , 2 mM NaH_2PO_4 , 1 mM Na_2EDTA , pH 7.0) containing 1.26 μM ethidium bromide were used to determine the C_{50} values for each compound. Apparent binding constants (K_{app}) were calculated as follows: $K_{\text{app}} = (1.26/C_{50}) \times K_{\text{ethidium}}$, with $K_{\text{ethidium}} = 10^7 \text{ M}^{-1}$. All measurements were carried out at room temperature with a Fluorolog spectrofluorimeter. The excitation and emission wavelengths were 546 nm and 595 nm, respectively (slit width: 10 nm). The experimental procedures for the electric linear dichroism¹³ and DNase I footprinting¹⁴ have been previously described.

Cell Culture and Growth Assays

Human prostate cancer PC 3 and DU 145 cells were maintained in RPMI 1640 culture medium supplemented with 10% FCS. For growth assays, the cells were seeded onto 96-well plates at a density of approximately 3×10^4 cells/well. After 3 days, the cell medium was changed to serum-free medium and the cells were starved for 24 h for culture synchronisation. Stimulation of the growth of quiescent cells was then provoked by 10 ng/ml EGF plus TSe (50 ng/ml transferrin and 50 pg/ml selenium) and the tested compounds were added to the culture medium. After an additional 72 h, cell growth was assessed by the colorimetric MTT test.

CHEMISTRY

The 9,11-dihydroindolizino[1,2-*b*]quinolines **10**, **11** were synthesized on the basis of the Friedländer reaction, requiring the appropriate 2-aminobenzaldehydes **3a**, **b** (and the imine surrogate **4**^{15,16}) and the enolizable indolizinsones **8** and **9** (Scheme 1).



SCHEME 1 Reagents and conditions: (i) *N*-2-chloroethylpiperidine, K₂CO₃, DMF, 80°C. (ii) Fe, HCl, AcOH, EtOH, H₂O, reflux. (iii) NaOH, MeOH, H₂O, reflux. (iv) Ni Raney, Ac₂O, AcOH, H₂, 45°C, 50 psi. (v) TFA 80%, rt. (vi) AcOH, reflux. (vii) 6 N HCl, reflux. ^aHydrochloride.

Aminobenzaldehydes were obtained in two steps by *O*-alkylation of phenols **1a**,¹⁷**b** (K₂CO₃, DMF) followed by the Bechamp reduction of the nitro group of **2a**,**b**. Indolizines **6** and **7** were synthesized from indolizine **5**.^{18,19} Carboxamide **6** was obtained by alkaline hydrolysis of the cyano group (without affecting the lactam moiety). These reaction conditions prevent over-hydrolysis of the carboxamide function into carboxylic acid. The protected amine **7** resulted from the catalytic hydrogenation of **5** in acylating medium. The protection of the amino group prevents a non-regioselective reaction during the Friedländer cyclisation. The acetal group in **5** was found essential to protect the ketone during the hydrogenation process. Deketalization of **6**, **7** enabled the Friedländer cyclisation^{20,21} of aldehydes **3a**,**b** (and **4**) with indolizines **8**, **9** to produce the tetracyclic compounds **10**, **11**; acetic acid acts as solvent and catalyst as well as a deprotective agent of the aldehydic function originating from **4**. Compounds **12a–c** were obtained from amides **11a–c** by classical acidic hydrolysis.

Materials

Melting points were determined with a Büchi 535 capillary melting point apparatus and are uncorrected. Analytical thin layer chromatography was performed on precoated Kieselgel 60F₂₅₄ plates (Merck); the spots were located by UV (254 and 366 nm); *R_f* values are given for guidance. Silica gel 60 230–400 Mesh (Merck) was used for column chromatography. The structures of most compounds

were supported by IR (KBr pellets, FT-Bruker Vector 22 instrument) and ¹H NMR at 300 MHz on a Bruker DRX-300 spectrometer. Chemical shifts were reported in ppm using tetramethylsilane (TMS) as a standard and the splitting patterns were designated as follows: s singlet, d doublet, t triplet, m multiplet. Mass spectra were recorded on a quadrupole Finnigan Mat SSQ 710 instrument. Elemental analyses were performed by the "Service Central d'Analyses" at the CNRS, Vernaison (France) and were within 0.4% of the calculated values. Commercially available reagents and solvents were used throughout without further purification.

2-Nitro-4-(2-piperidin-1-ylethoxy)benzaldehyde (**2a**) and 2-Nitro-5-(2-piperidin-1-ylethoxy)benzaldehyde (**2b**)

The phenol **1a**¹⁷ or **1b** (6 mmol) was added to a mixture of *N*-2-chloroethylpiperidine (1.1 g, 6 mmol), K₂CO₃ (2.5 g, 18 mmol) and DMF (10 mL) and heated while stirring to 80°C for 3 h. After cooling and dilution with H₂O (100 mL), the solution was extracted with Et₂O (3 × 100 mL). The combined organic phases were washed with saturated aqueous NaCl and dried (MgSO₄) before removal of the solvent. **2a**. Yellow oil (1.17 g, 70% yield). *R_f* = 0.78 (CH₂Cl₂/MeOH 9:1). IR (KBr), cm⁻¹: 1693 (C=O), 1536 (NO₂), 1351 (NO₂). ¹H NMR (CDCl₃), δ, ppm: 1.39 (m, 2H, H_{4'}), 1.55 (m, 4H, H_{3'}), 2.45 (m, 4H, H_{2'}), 3.28 (t, *J* = 6.0 Hz, 2H, NCH₂), 4.23 (t, *J* = 6.0 Hz, 2H, CH₂O), 7.18 (dd, *J_o* = 8.8 Hz, *J_m* = 2.7 Hz, 1H, H₅),

7.46 (d, $J_m = 2.8$ Hz, 1H, H₃), 8.22 (d, $J_o = 8.8$ Hz, 1H, H₆), 10.35 (s, 1H, CHO). **2b**. Yellow oil (1.50 g, 90% yield). $R_f = 0.47$ (CH₂Cl₂/MeOH 9:1). IR (KBr), cm⁻¹: 1698 (C=O), 1517 (NO₂), 1330 (NO₂). ¹H NMR (CDCl₃), δ , ppm: 1.41 (m, 2H, H₄'), 1.58 (m, 4H, H₃'), 2.48 (m, 4H, H₂'), 3.28 (t, $J = 5.8$ Hz, 2H, NCH₂), 4.21 (t, $J = 5.8$ Hz, 2H, CH₂O), 7.14 (dd, $J_o = 9.2$ Hz, $J_m = 2.9$ Hz, 1H, H₄), 7.30 (d, $J_m = 2.9$ Hz, 1H, H₆), 8.12 (d, $J_o = 9.2$ Hz, 1H, H₃), 10.44 (s, 1H, CHO).

2-Amino-4-(2-piperidin-1-ylethoxy)benzaldehyde (3a) and 2-Amino-5-(2-piperidin-1-ylethoxy)benzaldehyde (3b)

Nitrobenzaldehyde **2a** or **2b** (1 g, 3.6 mmol) was added to a mixture of iron (1.2 g, 21.6 mmol), 10 N HCl (0.25 mL), acetic acid (10 mL), ethanol (10 mL) and H₂O (5 mL), and heated while stirring under reflux for 15 min. Iron was removed by filtration and the filtrate was made alkaline with NaHCO₃ before extraction with CHCl₃ (3 × 70 mL). The combined extracts were dried (MgSO₄) and concentrated to give an oily residue. **3a**. Orange oil (670 mg, 75% yield). $R_f = 0.43$ (CH₂Cl₂/MeOH 9:1). IR (KBr), cm⁻¹: 3442 (NH₂), 3337 (NH₂), 1662 (C=O). ¹H NMR (CDCl₃), δ , ppm: 1.45 (m, 2H, H₄'), 1.61 (m, 4H, H₃'), 2.53 (m, 4H, H₂'), 2.78 (t, $J = 6.0$ Hz, 2H, NCH₂), 4.12 (t, $J = 6.0$ Hz, 2H, CH₂O), 6.08 (d, $J_m = 2.2$ Hz, 1H, H₃), 6.28 (dd, $J_o = 8.6$ Hz, $J_m = 2.2$ Hz, 1H, H₅), 6.31 (bs, 2H, NH₂), 7.33 (d, $J_o = 8.6$ Hz, 1H, H₆), 9.66 (s, 1H, CHO). **3b**. Brown oil (760 mg, 85% yield). $R_f = 0.36$ (CH₂Cl₂/MeOH 9:1). IR (KBr), cm⁻¹: 3441 (NH₂), 3332 (NH₂), 1664 (C=O). ¹H NMR (CDCl₃), δ , ppm: 1.46 (m, 2H, H₄'), 1.63 (m, 4H, H₃'), 2.56 (m, 4H, H₂'), 2.80 (t, $J = 5.8$ Hz, 2H, NCH₂), 4.10 (t, $J = 5.8$ Hz, 2H, CH₂O), 5.86 (bs, 2H, NH₂), 6.11 (d, $J_o = 8.6$ Hz, 1H, H₃), 6.99 (m, 1H, H₄), 7.03 (d, $J_m = 2.9$ Hz, 1H, H₆), 9.82 (s, 1H, CHO).

1,1-Ethylenedioxy-7-methyl-5-oxo-1,2,3,5-tetrahydroindolizine-6-carboxamide (6)

The nitrile **5**^{18,19} (2.0 g, 8 mmol) was added to a stirred solution of NaOH (3.3 g, 80 mmol) in H₂O (10 mL) and MeOH (50 mL) and the mixture was heated under reflux for 48 h. After cooling, acidification (CH₃COOH) and extraction with CH₂Cl₂ (3 × 100 mL), the combined extracts were dried (MgSO₄) and concentrated to give an oil which was precipitated from *i*Pr₂O. Recrystallization gave **6** as pale yellow crystals (1.4 g, 65% yield). $R_f = 0.65$ (CH₂Cl₂/MeOH 9:1). mp 187°C (toluene). IR (KBr), cm⁻¹: 3325 (NH₂), 3175 (NH₂), 1662 (C=O amide, pyridone). ¹H NMR (DMSO-*d*₆), δ , ppm: 2.32 (s, 3H, CH₃), 2.35 (t, $J = 7.0$ Hz, 2H, H₂), 3.94 (t, $J = 7.0$ Hz, 2H, H₃), 4.04–4.18 (m, 4H, OCH₂CH₂O), 6.36 (s, 1H, arom.), 7.37 (bs, 1H, CONH₂), 8.08 (bs, 1H, CONH₂).

N-(1,1-Ethylenedioxy-7-methyl-5-oxo-1,2,3,5-tetrahydroindolizine-6-ylmethyl)acetamide (7)

The hydrogenation of **5** (1.0 g, 3.6 mmol), dissolved in acetic anhydride (45 mL) and acetic acid (15 mL), was carried out on a Parr apparatus (Raney nickel 1.5 g, 50 psi, 45°C, 6 h) followed by filtration of the catalyst and evaporation of the solvent under reduced pressure. The residue was diluted in H₂O (100 mL), then extracted with CHCl₃ (3 × 100 mL). The organic layer was dried (MgSO₄) and the resulting oil was crystallized from Et₂O to yield **7** as a white solid (860 mg, 72% yield). $R_f = 0.55$ (CH₂Cl₂/MeOH 9:1). mp 152°C. IR (KBr), cm⁻¹: 3258 (NH), 1656 (C=O amide, pyridone). ¹H NMR (CDCl₃), δ , ppm: 1.93 (s, 3H, COCH₃), 2.36 (t, $J = 6.6$ Hz, 2H, H₂), 2.40 (s, 3H, CH₃), 4.07–4.18 (m, 6H, OCH₂CH₂O, H₃), 4.36 (d, $J = 6.0$ Hz, 2H, CH₂N), 6.14 (s, 1H, arom.), 6.81 (bs, 1H, NH).

General Procedure for the Synthesis of 7-Methyl-1,5-dioxo-1,2,3,5-tetrahydroindolizine-6-carboxamide (8) and N-(7-Methyl-1,5-dioxo-1,2,3,5-tetrahydroindolizine-6-ylmethyl)acetamide (9)

A solution of **6** or **7** (4 mmol) in 80% aqueous TFA (10 mL) was stirred at room temperature for 3 h in a nitrogen atmosphere. Removal of the solvent gave an oil which crystallized from Et₂O.

8. Yellow solid (715 mg, 85% yield). $R_f = 0.38$ (CH₂Cl₂/MeOH 9:1). mp 185°C. IR (KBr), cm⁻¹: 3301 (NH), 1735 (C=O ketone) 1647 (C=O amide, pyridone). ¹H NMR (DMSO-*d*₆), δ , ppm: 2.31 (s, 3H, CH₃), 2.88 (t, $J = 6.5$ Hz, 2H, H₂), 4.08 (t, $J = 6.5$ Hz, 2H, H₃), 6.75 (s, 1H, arom.), 7.53 (bs, 1H, CONH₂), 7.99 (bs, 1H, CONH₂).

9. Pale yellow solid (770 mg, 93% yield). $R_f = 0.46$ (CH₂Cl₂/MeOH 9:1). mp 161°C. IR (KBr), cm⁻¹: 3328 (NH₂), 3130 (NH₂), 1745 (C=O ketone), 1672 (C=O amide, pyridone). ¹H NMR (CDCl₃), δ , ppm: 1.95 (s, 3H, COCH₃), 2.51 (s, 3H, CH₃), 2.91 (t, $J = 6.6$ Hz, 2H, H₂), 4.29 (t, $J = 6.6$ Hz, 2H, H₃), 4.42 (d, $J = 6.6$ Hz, 2H, CH₂N), 6.80 (m, 2H, NH, arom.).

General Procedure for the Synthesis of 9,11-Dihydroindolizino[1,2-*b*]quinolines 10a–c and 11a–c

Tetrahydroindolizine **8** or **9** and 2-aminobenzaldehyde **3a**, **3b** or **4**^{12,13} were added to acetic acid (20 mL) and heated while stirring under reflux for 8 h. The reaction mixture was cooled to room temperature and the solvent was removed under reduced pressure. The crude product was diluted in methanol and hydrogen chloride was bubbled through. The products were purified by flash chromatography (CH₂Cl₂–MeOH 8/2 → 7/3) before recrystallization.

7-Methyl-9-oxo-3-(2-piperidin-1-ylethoxy)-9,11-dihydroindolizino[1,2-*b*]quinoline-8-carboxamide Hydrochloride (10a)

Pale yellow solid (340 mg, 51% yield) from **8** (320 mg, 1.6 mmol) and **3a** (385 mg, 1.6 mmol). $R_f = 0.31$ (CH₂Cl₂/MeOH 9:1, ammonia 1%). mp > 250°C (EtOH/H₂O). IR (KBr), cm⁻¹: 3300 (NH), 1676 (C=O pyridone, amide), 1619 (C=N). ¹H NMR (DMSO-*d*₆), δ, ppm: 1.42 (m, 2H, H₄), 1.82 (m, 4H, H₃), 2.50 (s, 3H, CH₃), 3.05 (m, 2H, NCH₂), 3.59 (m, 4H, H₂), 4.63 (m, 2H, CH₂O), 5.23 (s, 2H, H₁₁), 7.10 (s, 1H, H₆), 7.42 (dd, $J_o = 9.1$ Hz, $J_m = 2.3$ Hz, 1H, H₂), 7.49 (bs, 1H, CONH₂), 7.60 (d, $J_m = 2.3$ Hz, 1H, H₄), 8.09 (d, $J_o = 9.1$ Hz, 1H, H₁), 8.24 (bs, 1H, CONH₂), 8.64 (s, 1H, H₁₂), 10.22 (bs, 1H, NH⁺). Anal. Calcd. for C₂₄H₂₆N₄O₃•1HCl•2.5H₂O: C, 57.65; H, 6.45; N, 11.21; Cl, 17.09. Found: C, 57.89; H, 6.20; N, 11.53; Cl, 17.11%.

7-Methyl-9-oxo-2-(2-piperidin-1-ylethoxy)-9,11-dihydroindolizino[1,2-*b*]quinoline-8-carboxamide Hydrochloride (10b)

Pale yellow solid (330 mg, 49% yield) from **8** (320 mg, 1.6 mmol) and **3b** (385 mg, 1.6 mmol). $R_f = 0.48$ (CH₂Cl₂/MeOH 9:1, ammonia 1%). mp > 250°C (EtOH/H₂O). IR (KBr), cm⁻¹: 3360 (NH), 1658 (C=O pyridone, amide). ¹H NMR (DMSO-*d*₆), δ, ppm: 1.71 (m, 2H, H₄), 1.82 (m, 4H, H₃), 2.49 (s, 3H, CH₃), 3.06 (m, 2H, NCH₂), 3.56 (m, 4H, H₂), 4.60 (m, 2H, CH₂O), 5.23 (s, 2H, H₁₁), 7.11 (s, 1H, H₆), 7.48 (bs, 1H, CONH₂), 7.55 (dd, $J_o = 9.2$ Hz, $J_m = 2.7$ Hz, 1H, H₃), 7.61 (d, $J_m = 2.7$ Hz, 1H, H₁), 8.08 (d, $J_o = 9.2$ Hz, 1H, H₄), 8.28 (bs, 1H, CONH₂), 8.56 (s, 1H, H₁₂), 10.35 (bs, 1H, NH⁺). Anal. Calcd. for C₂₄H₂₆N₄O₃•1HCl•2.5H₂O: C, 57.65; H, 6.45; N, 11.21; Cl, 17.09. Found: C, 57.60; H, 6.34; N, 11.19; Cl, 17.31%.

7-Methyl-9-oxo-9,11-dihydroindolizino[1,2-*b*]quinoline-8-carboxamide (10c)

Brown solid (290 mg, 42% yield) from **8** (500 mg, 2.4 mmol) and **4** (510 mg, 2.4 mmol). $R_f = 0.49$ (CH₂Cl₂/MeOH 9:1, ammonia 1%). mp > 250°C (EtOH/H₂O). IR (KBr), cm⁻¹: 3275 (NH), 1668 (C=O pyridone, amide). ¹H NMR (DMSO-*d*₆), δ, ppm: 2.51 (s, 3H, CH₃), 5.28 (s, 2H, H₁₁), 7.21 (s, 1H, H₆), 7.51 (bs, 1H, CONH₂), 7.73 (td, $J_o = 8.3$ Hz, $J_m = 1.3$ Hz, 1H, H₂ or ₃), 7.88 (td, $J_o = 8.3$ Hz, $J_m = 1.3$ Hz, 1H, H₂ or ₃), 8.17 (m, 2H, H₁, H₄), 8.24 (bs, 1H, CONH₂), 8.72 (s, 1H, H₁₂). Anal. Calcd. for C₁₇H₁₃N₃O₂•0.5HCl•0.5H₂O: C, 64.09; H, 4.59; N, 13.19. Found: C, 64.31; H, 4.30; N, 13.03%.

***N*-[7-Methyl-9-oxo-3-(2-piperidin-1-ylethoxy)-9,11-dihydroindolizino[1,2-*b*]quinolin-8-ylmethyl]acetamide Hydrochloride (11a)**

Orange solid (1.0 g, 45% yield) from **3a** (1.2 g, 5 mmol) and **9** (1.2 g, 5 mmol). $R_f = 0.39$ (CH₂Cl₂/MeOH 9:1, ammonia 1%). mp > 250°C (EtOH/H₂O). IR (KBr), cm⁻¹: 3300 (NH), 1664 (C=O pyridone, amide), 1618 (C=N). EI MS m/z (relative intensity) 446 (M⁺, 14%), 403 (M⁺-COCH₃, 22%), 304 (M⁺-COCH₃-piperidine, 17%), 275 (M⁺-COCH₃-piperidine-CH₂NH, 14%).

***N*-[7-Methyl-9-oxo-2-(2-piperidin-1-ylethoxy)-9,11-dihydroindolizino[1,2-*b*]quinolin-8-ylmethyl]acetamide Hydrochloride (11b)**

Brown solid (1.0 g, 44% yield) from **3b** (1.2 g, 5 mmol) and **9** (1.2 g, 5 mmol). $R_f = 0.22$ (CH₂Cl₂/MeOH 9:1, ammonia 1%). mp > 250°C (EtOH/H₂O). IR (KBr), cm⁻¹: 3418 (NH), 1655 (C=O pyridone, amide), 1621 (C=N). EI MS m/z (relative intensity) 446 (M⁺, 15%), 403 (M⁺-COCH₃, 20%), 304 (M⁺-COCH₃-piperidine, 8%), 275 (M⁺-COCH₃-piperidine-CH₂NH, 6%).

***N*-[7-Methyl-9-oxo-9,11-dihydroindolizino[1,2-*b*]quinolin-8-ylmethyl]acetamide (11c)**

Brown solid (290 mg, 48% yield) from **4** (450 mg, 1.9 mmol) and **9** (400 mg, 1.9 mmol). $R_f = 0.63$ (CH₂Cl₂/MeOH 9:1, ammonia 1%). mp > 250°C (EtOH/H₂O). IR (KBr), cm⁻¹: 3329 (NH), 1666 (C=O pyridone, amide). EI MS m/z (relative intensity) 319 (M⁺, 10%), 276 (M⁺-COCH₃, 100%).

General Procedure for the Synthesis of 9,11-Dihydroindolizino[1,2-*b*]quinolines 12a–c

Quinoline **11a**, **11b** or **11c** was added to 6 N HCl and heated while stirring under reflux for 24 h. After cooling to room temperature and removal of the solvent under reduced pressure, the crude product was purified by flash chromatography (CH₂Cl₂-MeOH 7/3).

8-Aminomethyl-7-methyl-9-oxo-3-(2-piperidin-1-ylethoxy)-9,11-dihydroindolizino[1,2-*b*]quinoline Dihydrochloride (12a)

Yellow solid (130 mg, 76% yield) from **11a** (150 mg, 3.4 mmol) and HCl (15 mL). $R_f = 0.39$ (CH₂Cl₂/MeOH 9:1, ammonia 1%). mp > 250°C (EtOH/H₂O). IR (KBr), cm⁻¹: 3386 (NH₃⁺), 1653 (C=O), 1617 (C=N). ¹H NMR (DMSO-*d*₆), δ, ppm: 1.70 (m, 2H, H₄), 1.83 (m, 4H, H₃), 2.46 (s, 3H, CH₃), 3.05 (m, 2H, NCH₂), 3.58 (m, 4H, H₂), 3.98 (s, 2H, CH₂N), 4.68 (m, 2H, CH₂O), 5.26 (s, 2H,

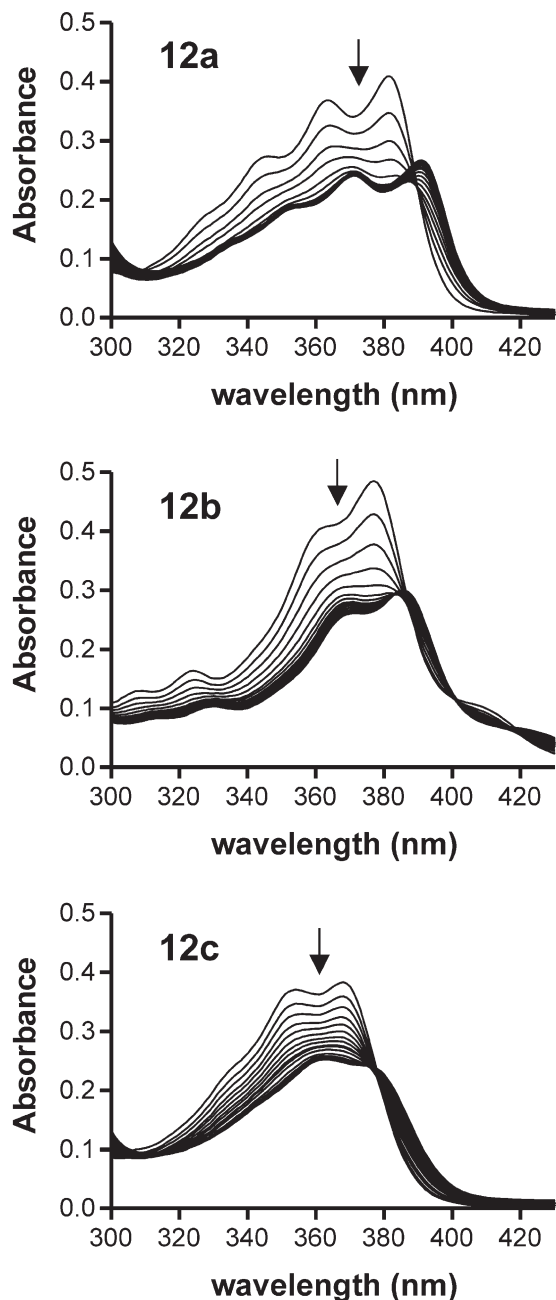


FIGURE 3 Absorption spectral changes on titration of compounds **12a–c** with DNA. To 3 mL of drug solution at 20 μM were added aliquots of a concentrated calf thymus DNA solution. The phosphate-DNA/drug ratio increased from 0 to 10 (top to bottom curves, at 380 nm). Measurements were performed in 1 mM sodium cacodylate buffer, pH 7.0.

H_{11}), 7.16 (s, 1H, H_6), 7.43 (dd, $J_o = 9.1$ Hz, $J_m = 2.0$ Hz, 1H, H_2), 7.58 (d, $J_m = 2.0$ Hz, 1H, H_4), 8.08 (d, $J_o = 9.1$ Hz, 1H, H_1), 8.23 (bs, 3H, NH_3^+), 8.65 (s, 1H, H_{12}), 10.85 (bs, 1H, NH^+). Anal. Calcd. for $\text{C}_{24}\text{H}_{28}\text{N}_4\text{O}_2 \cdot 2\text{HCl} \cdot 3\text{H}_2\text{O}$: C, 54.24; H, 6.83; N, 10.54; Cl, 13.34. Found: C, 53.94; H, 6.63; N, 10.52; Cl, 13.26%.

TABLE I DNA binding parameters

	ΔT_m ($^\circ\text{C}$)		Abs*		K_{app}^{\dagger} $\times 10^6$ (M^{-1})
	CT	dAT	$\Delta\lambda$	H	
10a	4.6	12.8	8	35.8	0.200 ± 0.002
10b	1.2	5.8	9	33.0	0.290 ± 0.003
10c	0	0	0	2.7	– [‡]
12a	19.4	28.6	11	38.6	8.40 ± 0.12
12b	13.6	19.8	9	35.3	2.50 ± 0.08
12c	1.9	3	8	33.1	– [‡]

* Absorption spectral changes recorded on addition of 200 μM calf thymus DNA to a drug solution at 20 μM in 1 mM Na cacodylate buffer, pH 7.0. H and $\Delta\lambda$ refer to the hypochromic (%) and bathochromic (nm) shifts.

[†] Binding constants calculated from the concentration required to reduce by 50% the fluorescence of ethidium bromide bound to calf thymus DNA. [‡] No displacement of DNA-bound ethidium bromide at 50 μM .

8-Aminomethyl-7-methyl-9-oxo-2-(2-piperidin-1-ylethoxy)-9,11-dihydroindolizino [1,2-b]quinoline Dihydrochloride (**12b**)

Yellow solid. (150 mg, 70% yield) from **11b** (200 mg, 4.4 mmol) and HCl (20 mL). $R_f = 0.36$ ($\text{CH}_2\text{Cl}_2/\text{MeOH}$ 9:1, ammonia 1%). mp > 250 $^\circ\text{C}$ ($\text{EtOH}/\text{H}_2\text{O}$). IR (KBr), cm^{-1} : 3417 (NH_3^+), 1655 (C=O), 1621 (C=N). ^1H NMR ($\text{DMSO}-d_6$), δ , ppm: 1.71 (m, 2H, H_4), 1.87 (m, 4H, H_3), 2.46 (s, 3H, CH_3), 3.07 (m, 2H, NCH_2), 3.55 (m, 4H, H_2), 4.00 (s, 2H, CH_2N), 4.68 (m, 2H, CH_2O), 5.27 (s, 2H, H_{11}), 7.15 (s, 1H, H_6), 7.57 (d, $J_o = 9.0$ Hz, 1H, H_3), 7.64 (s, 1H, H_1), 8.09 (d, $J_o = 9.0$ Hz, 1H, H_4), 8.23 (bs, 3H, NH_3^+), 8.57 (s, 1H, H_{12}), 11.27 (bs, 1H, NH^+). Anal. Calcd. for $\text{C}_{24}\text{H}_{28}\text{N}_4\text{O}_2 \cdot 2\text{HCl} \cdot 3.5\text{H}_2\text{O}$: C, 53.33; H, 6.90; N, 10.37; Cl, 13.12. Found: C, 53.52; H, 6.75; N, 10.30; Cl, 12.96%.

8-Aminomethyl-7-methyl-9-oxo-9,11-dihydroindolizino[1,2-b]quinoline Hydrochloride (**12c**)

Pale yellow solid (850 mg, 58% yield) from **11c** (150 mg, 4.7 mmol) and HCl (15 mL). $R_f = 0.59$ ($\text{CH}_2\text{Cl}_2/\text{MeOH}$ 9:1, ammonia 1%). mp > 250 $^\circ\text{C}$ ($\text{EtOH}/\text{H}_2\text{O}$). IR (KBr), cm^{-1} : 3422 (NH_3^+), 1656 (C=O), 1609 (C=N). ^1H NMR ($\text{DMSO}-d_6$), δ , ppm: 3.35 (s, 3H, CH_3), 4.00 (s, 2H, CH_2N), 5.31 (s, 2H, H_{11}), 7.27 (s, 1H, H_6), 7.74 (td, $J_o = 8.3$ Hz, $J_m = 1.3$ Hz, 1H, H_2 or 3), 7.88 (td, $J_o = 8.3$ Hz, $J_m = 1.3$ Hz, 1H, H_2 or 3), 8.09 (bs, 3H, NH_3^+), 8.15–8.18 (m, 2H, H_1 , H_4), 8.72 (s, 1H, H_{12}). Anal. Calcd. for $\text{C}_{17}\text{H}_{15}\text{N}_3\text{O} \cdot 1.5\text{HCl} \cdot 2.25\text{H}_2\text{O}$: C, 54.81; H, 5.68; N, 11.28; Cl, 14.27. Found: C, 54.43; H, 5.38; N, 11.13; Cl, 14.27%.

RESULTS AND DISCUSSION

DNA Interaction

Addition of DNA induces marked changes to the absorption spectra of the compounds **12a–c** (Figure 3).

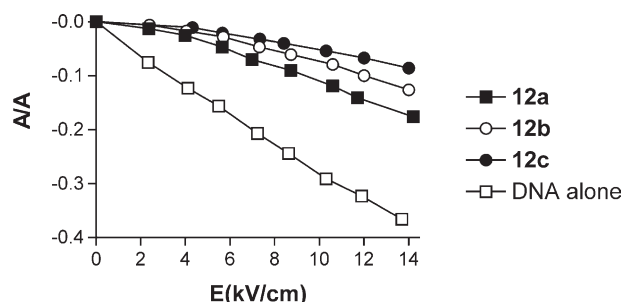


FIGURE 4 Dependence of reduced dichroism $\Delta A/A$ on the electric field strength for compounds **12a–c** bound to calf thymus DNA. Conditions: P/D = 25 (250 μM DNA, 10 μM drug), 389 nm for **12a**, 383 nm for **12b**, 366 nm for **12c**, and 260 nm for DNA alone. Measurements were performed in 1 mM sodium cacodylate buffer, pH 7.0.

Good isosbestic behaviour is observed with these compounds. With **12a**, the absorption maximum is shifted from 381 to 392 nm and the red-shift amounts to 9 nm with **12b** (from 377 to 386 nm) (Table I). An important hypochromic shift is also seen: H = 38.6% for **12a** (Table I). The amide compounds **10a–c** showed weaker spectral changes compared to the aminomethyl analogues (Table I).

The interaction of the drugs with DNA was also investigated by thermal denaturation analysis to estimate their relative affinity. The T_m measurements, carried out with calf thymus DNA and the polynucleotide poly(dAT)₂, gave the ΔT_m values ($\Delta T_m = T_m^{\text{complex}} - T_m^{\text{DNA}}$) collected in Table I. There were great differences between the compounds. In the aminomethyl series, **12a,b** stabilized duplex DNA against heat denaturation much more strongly than **12c**, indicating that the side chain played a significant role in drug-DNA interaction.

The position of the side chain on the chromophore was also important because with both calf thymus DNA and poly(dAT)₂, the T_m shifts were more pronounced with **12a** than with **12b**. The side chain introduced on the chromophore at position-3 was preferable to position-2.

Binding affinities were determined by fluorescence using an ethidium bromide-displacement assay. **12a** was found to bind strongly to calf thymus DNA with an apparent binding constant about 4 times higher than that determined for **12b** and 40 times superior to those calculated for the amides **10a,b** (Table I).

The binding mode of **12a–c** to DNA was probed by electric linear dichroism (ELD) using calf thymus DNA and the polynucleotides poly(dA–dT)₂ and poly(dG–dC)₂ (Figure 4). In all cases, the reduced dichroism $\Delta A/A$ was negative in the drug absorption band, which reflects the orientation of the chromophore perpendicular to the helix axis, as expected for an intercalative binding. Unwinding of supercoiled DNA was observed with **12a**, confirming that this compound is a DNA intercalator.

DNA Sequence Recognition

Footprinting experiments were performed with four restriction fragments (Figure 5).

The DNA substrates, 3'-end radiolabeled, were incubated with increasing concentrations of **12a–c** and, after equilibration, the complexes were subjected to limited cleavage by DNase I. Clear modifications in the patterns of cleavage by DNase I were observed with **12a** whereas **12b** and **12c** showed little, if any, effect on enzyme activity.

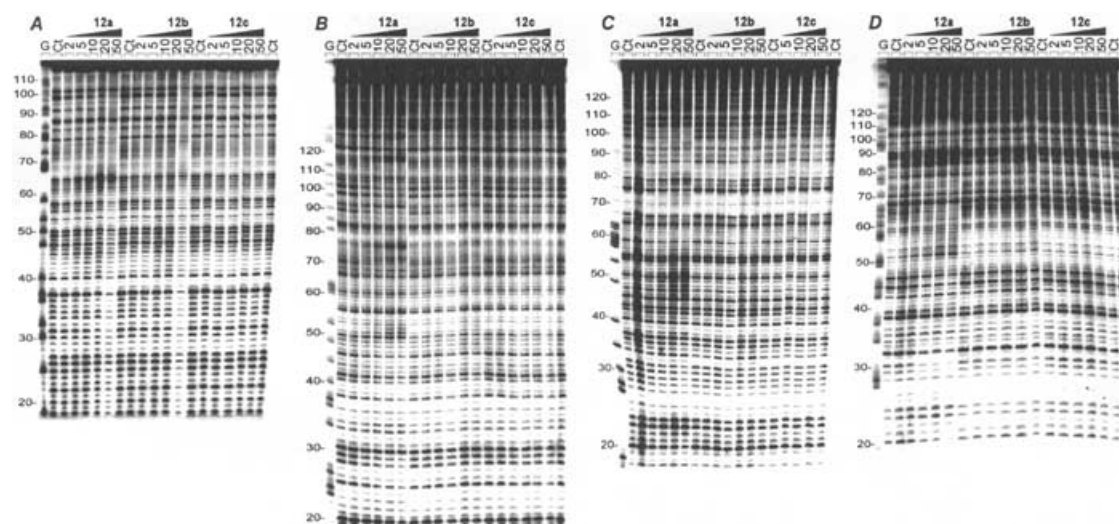


FIGURE 5 DNase I footprinting of **12a–c** on the (A) 117-bp and (B) 265-bp *EcoRI-PvuII* fragments from pBS and the *HindIII-XbaI* 198-bp (C) MS1 and (D) MS2 fragments. In each case, the DNA was 3'-end labeled with [α -³²P]dATP in the presence of AMV reverse transcriptase. The products of nuclease digestion were resolved on an 8% polyacrylamide gel containing 8 M urea. The concentration (μM) of the drug is shown at the top of the appropriate gel lanes. Control tracks (Ct) contained no drug. Tracks labeled "G" represent dimethylsulphate-piperidine markers specific for guanines.

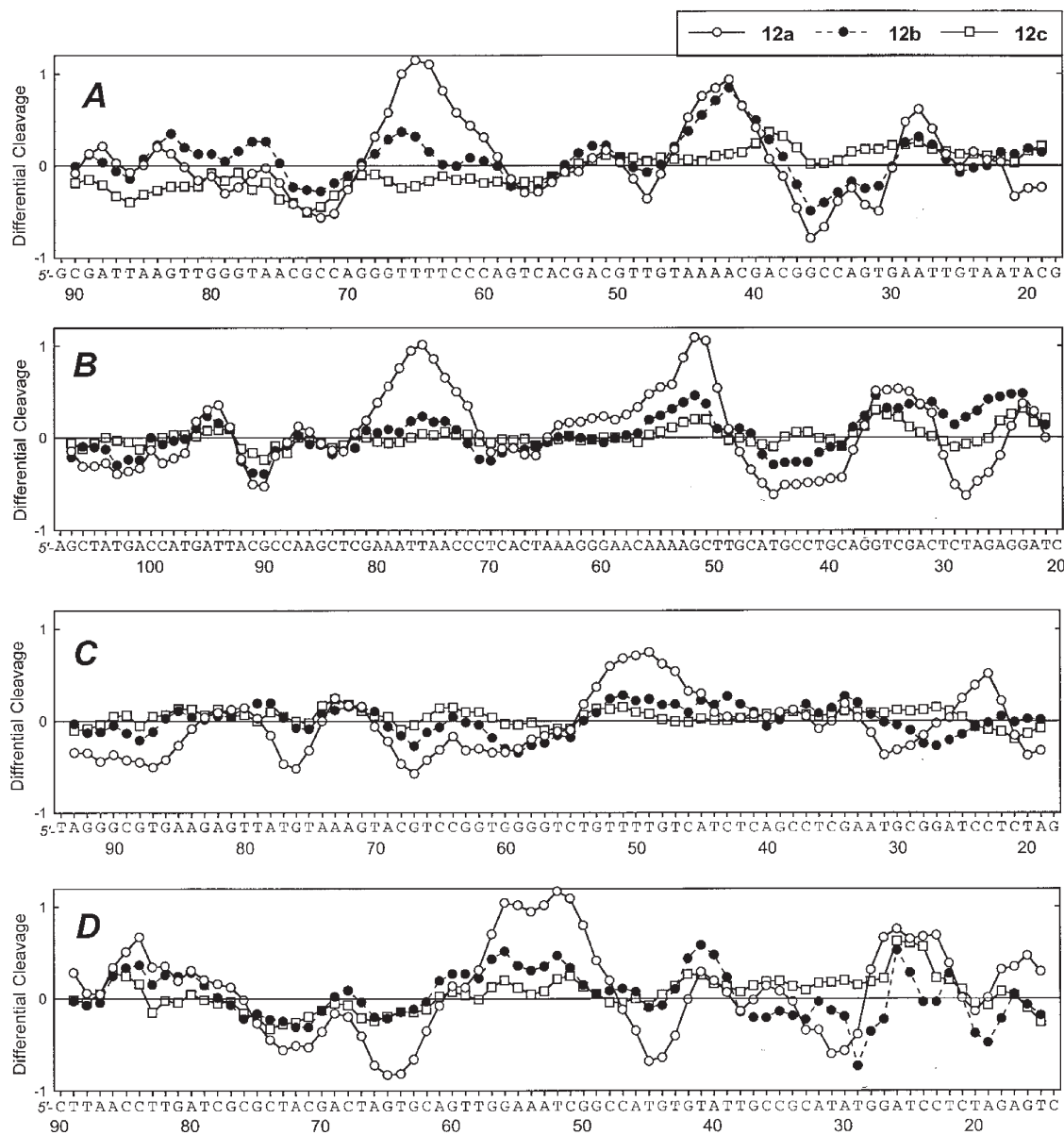


FIGURE 6 Differential cleavage plots comparing the susceptibility of (A) the 117-mer and (B) 265-mer DNA fragments to DNase I cutting in the presence of the compounds (20 μ M each). Panels (C) and (D) show the differential cleavage plots for the drugs bound to the 198-bp DNA fragments MS1 and MS2 containing the cloned sequence which constitutes all 136 distinguishable tetranucleotide sequences. Negative values correspond to a ligand-protected site and positive values represent enhanced cleavage. Vertical scales are in units of $\ln(f_a) - \ln(f_c)$, where f_a is the fractional cleavage at any bond in the presence of the drug and f_c is the fractional cleavage of the same bond in the control, given closely similar extents of overall digestion. Each line drawn represents a 3-bond running average of individual data points, calculated by averaging the value of $\ln(f_a) - \ln(f_c)$ at any bond with those of its nearest two neighbours. Only the region of the restriction fragment analyzed by densitometry is shown.

A few sites of protection from DNase I cutting (i.e. footprints) adjacent to regions of enhanced cleavage can be detected with **12a** as the ligand concentration is raised, but not with **12b,c**. The gels were analyzed by phosphor imaging to determine the exact position of the footprints, presumptive ligand binding sites. A range of binding sequences were identified from differential cleavage plots (Figure 6).

12a was found to bind selectively to many sequences with a high GC content, such as

5'-GGCCAGT, 5'-CGCC, 5'-TCTAGA, 5'-CATGCTGC, 5'-GCGTG and 5'-ACGC. Binding to a few AT/GC mixed sequences, such as 5'-ACGT, 5'-AGTG, 5'-CTAC and 5'-ATGT, was also detected. On the contrary, DNase I cutting at AT-rich sequences was found to be enhanced in the presence of **12a** and this effect can be attributed to intercalation-induced perturbations of the double helical structure of DNA. It appears that **12a** is sensitive to GC-rich sequences and those containing GpT (ApC) and TpG (CpA) steps.

TABLE II IC₅₀ against DU 145 and PC 3, two human prostatic cancer cell lines

	IC ₅₀ DU 145 (μM)	IC ₅₀ PC 3 (μM)
10a	> 50	> 50
10b	> 50	> 50
10c	> 50	6.7
12a	6.2	4.6
12b	11.8	11.0
12c	> 50	> 50
CPT ²²	ND	0.06
TPT ^{22,23}	0.04	0.16

Cytotoxicity Assays

The results on *in vitro* cytotoxicity bioassays are shown in Table II.

Compounds **12a,b** with an aminomethyl group on ring D and a piperidine side chain on the A-ring showed a modest anti-proliferative activity whereas **12c**, without a side chain did not show any activity. **12a**, with the side chain at position-3, had an IC₅₀ of 4.6 μM on PC 3 and was twice as potent as **12b**.

Compounds **10a–c** with an aminocarbonyl group on ring D were poorly active or inactive. Only **10c**, without a side chain on ring A, had an IC₅₀ of 6.7 μM on PC 3. This compound had a poor affinity for DNA (Table I), so it may be supposed that DNA-binding was not required to induce cell death.

All of these compounds present a weak cytotoxicity on PC 3 and DU 145 cells, compared with those of CPT and TPT (Figure 1). It can be concluded that the E-ring deletion is critical for the cytotoxicity.

CONCLUSION

This study shows that the A–D ring subunit of CPT is particularly well adapted for potent and selective recognition of GC-rich DNA sequences. The DNA binding data can be rationalized by a model in which the indolizino[1,2-*b*]quinoline chromophore stacks on a G•C pair. Incorporation of a cationic piperidino-ethyloxy side chain significantly reinforces DNA interaction. Moreover this chain gives better interaction when introduced in position-3 rather than -2. These compounds have weak cytotoxicity on human prostate cancer cell lines PC 3 and DU 145. The present data also provides important information for understanding more fully the mechanism of action of indolizino[1,2-*b*]quinolines such as batracyclins which are highly potent antitumor agents.²⁴

Acknowledgements

This work was supported by research grants (to Christian Bailly and Jean-Pierre Hélichart) from

the Association pour la Recherche sur le Cancer and (to Claude Houssier and Pierre Colson) from the Actions de Recherches Concertées 95/00-93 and from "Actions intégrées Franco-Belges, Programme Tournesol".

References

- [1] Govindachari, T.R., Ravindranath, K.R. and Viswanathan, N. (1974) *J. Chem. Soc. Perkin Trans. 1*, 1215–1217.
- [2] Pendrak, I., Barney, S., Wittrock, R., Lambert, D.M. and Kingsbury, W.D. (1994) *J. Org. Chem.* **59**, 2623–2625.
- [3] Pendrak, I., Wittrock, R. and Kingsbury, W.D. (1995) *J. Org. Chem.* **60**, 2912–2915.
- [4] Wall, M.E., Wani, M.C., Cook, C.E., Palmer, K.H., Mc Phail, A.T. and Sim, G.A. (1966) *J. Am. Chem. Soc.* **88**, 3888–3890.
- [5] Pommier, Y., Pourquier, P., Fan, Y. and Strumberg, D. (1998) *Biochim. Biophys. Acta* **1400**, 83–106.
- [6] Fan, Y., Weinstein, J.N., Kohn, K.W., Shi, L.M. and Pommier, Y. (1998) *J. Med. Chem.* **41**, 2216–2226.
- [7] Redinbo, M.R., Stewart, L., Kuhn, P., Champoux, J.J. and Hol, W.G.J. (1998) *Science* **279**, 1504–1513.
- [8] Redinbo, M.R., Champoux, J.J. and Hol, W.G.J. (2000) *Biochemistry* **39**, 6832–6840.
- [9] Kerrigan, J.E. and Pilch, D.S. (2001) *Biochemistry* **40**, 9792–9798.
- [10] Laco, G.S., Collins, J.R., Luke, B.T., Kroth, H., Sayer, J.M., Jerina, D.M. and Pommier, Y. (2002) *Biochemistry* **41**, 1428–1435.
- [11] Goossens, J.-F., Bouey-Bencteux, E., Houssier, R., Hélichart, J.-P., Colson, P., Houssier, C., Laine, W., Baldeyrou, B. and Bailly, C. (2001) *Biochemistry* **40**, 4663–4671.
- [12] Baguley, B.C., Denny, W.A., Atwell, G.J. and Cain, B.F. (1981) *J. Med. Chem.* **24**, 170–177.
- [13] Colson, P., Bailly, C. and Houssier, C. (1996) *Biophys. Chem.* **58**, 125–140.
- [14] Bailly, C., Goossens, J.-F., Laine, W., Anizon, F., Prudhomme, M., Ren, J. and Chaires, J.B. (2000) *J. Med. Chem.* **43**, 4711–4720.
- [15] Borsche, W., Doeller, W. and Wagner-Roemmich, M. (1943) *Chem. Ber.* **76**, 1099–1102.
- [16] Johnston, D., Smith, D.M., Shepherd, T. and Thompson, D. (1987) *J. Chem. Soc. Perkin Trans. 1*, 495–500.
- [17] Suvorov, N.N., Fedotova, M.V., Orlova, L.M. and Ogareva, O.B. (1962) *J. Gener. Chem. USSR (English Translation)* **32**, 2325–2331.
- [18] Wani, M.C., Ronman, P.E., Lindley, J.T. and Wall, M.E. (1980) *J. Med. Chem.* **23**, 554–560.
- [19] Wall, M.E. and Wani, M. (1991) "PCT Int. Appl. WO 91/05556", *Chem. Abst.* **115**, 92686x.
- [20] Sugimori, M., Ejima, A., Ohsuki, S., Uoto, K., Mitsui, I., Matsumoto, K., Kawato, Y., Hirota, Y., Sato, K. and Terasawa, H. (1998) *J. Med. Chem.* **41**, 2308–2318.
- [21] Cheng, C.C. and Yan, S.J. (1982) In: Bittman, R., Boswell, G.A., Danishefsky, S., Dauben, W.G., Gschwend, H.W., Heck, R.F., Hirschmann, R.F., Kende, A.S., Paquette, L.A., Posner, G.H., Trost, B.M. and Weinstein, B. eds, *Organic Reactions* (Wiley, New York) **28**, pp 37–201.
- [22] Lavergne, O., Lesueur-Ginot, L., Pla Rodas, F., Kasprzyk, P.G., Pommier, J., Demarquay, D., Prévost, G., Ulibarri, G., Rolland, A., Schiano-Liberatore, A.M., Harnett, J., Pons, D., Camara, J. and Bigg, D.C.H. (1998) *J. Med. Chem.* **41**, 5410–5419.
- [23] Subrahmanyam, D., Venkateswarlu, A., Venkateswara Rao, K., Sastry, T., Vandana, G. and Kumar, S.A. (1999) *Bioorg. Med. Chem. Lett.* **9**, 1633–1638.
- [24] Wang, H.-K., Morris-Natschke, S.L. and Lee, K.-H. (1997) *Med. Res. Rev.* **17**, 367–425.

Copyright of Journal of Enzyme Inhibition & Medicinal Chemistry is the property of Taylor & Francis Ltd and its content may not be copied or emailed to multiple sites or posted to a listserv without the copyright holder's express written permission. However, users may print, download, or email articles for individual use.